SF2A 2024
M. Béthermin, K. Baillié, N. Lagarde, J. Malzac, R.-M. Ouazzani, J. Richard, O. Venot, A. Siebert (eds)

NEW RADIATIVE TRANSFER METHODS IN NUMERICAL SIMULATIONS OF GALAXY FORMATION: APPLICATION TO THE EPOCH OF REIONIZATION

M. Palanque[1], P. Ocvirk[1], E. Franck[2] and P. Gerhard[3]

Abstract. Most current reionisation epoch simulations use the same model for radiative transfer, the moment model M1. However, despite its low computational cost, this model comes with approximations that could change the output of the simulations and alter our understanding of the epoch of reionization; for example, as M1 approximates photons as a fluid, two colliding fronts of photon waves tend to create pseudo sources that should not exist. We implemented and compared competing models of radiative transfer, mainly the Pn model, to see if it could be a replacement or a complementary model to M1. We observe that it solves the issue of pseudo sources in colliding fronts, though at a greater computational cost. Since Pn does not guarantee the positivity of the energy, special care must be taken in the photo-chemistry steps. We perform a number of standard tests demonstrating the correct general behaviour of our Pn solver, and better directionality than M1. It is therefore a promising development provided the higher computational cost can be accommodated.

Keywords: Reionisation, radiative transfer, Pn

1 Introduction

The epoch of reionization takes place starting 150 My after the big bang, and ends approximately around 1 Gyr after the big bang (redshift 20 to 6). During this period of our universe's history, its entire gas content gets ionised by the recently formed galaxies and stars. However, details about how this reionization took place are still debated, and observational constraints for this period, such as the ones that will be brought by SKA, are still a long way from now. Numerical simulations may offer insight into the epoch of reionization and help us prepare future observational campaigns. Radiative transfer is a central component of reionisation epoch simulations, since it is through ionising rays that the ionised fraction of hydrogen is computed. The ionisation of the intergalactic medium (IGM) being the main subject of study of this epoch, the need for a reliable radiative transfer model is central to better describe this process. The most commonly used model nowadays, called M1, is a moment derived model with an analytic closure relation, which allows great approximation in a reasonable computing time. However, M1 isn't without flaws, as, for example, its directionality tends to create pseudo-sources at the colliding point of two wave fronts. This could be one of the reasons why it tends to under estimate the photo-ionisation rate at small scales (Wu et al. 2021), but, at this point, we don't really know what could be the scale of the effects of this property of the M1 model on the results of numerical simulations.

We aim at comparing the M1 closure (Aubert & Teyssier 2008) to other commonly used models of the literature (Garrett & Hauck 2013), especially the Pn model and its variations. The objective is determining if Pn can correct M1's flaws while being as good as it on subject where M1 already performs well. We'll also be comparing computational costs.

[1] Observatoire de Strasbourg
[2] IRMA, Strasbourg
[3] DNum, Strasbourg

2 The Pn model

2.1 Implementation

The Pn Model (Meltz 2015) is a moment derived model just like M1, but based on an angular spectral decomposition projected on spherical harmonics. It's closure relation at order n simply ignores all moments of order superior or equal to $n+1$. This peculiar closure relation allows to derive further than order 1 as M1 does.

Moments derived model work by computing a certain number of moments of the radiative transfer equation until the closure relation. The number of moment coefficients to be computed for a given order n is $(n+1)^2$. Thus, if the M1 model only requires the computation of 4 coefficients per cell, models such as P9 will require up to 100 coefficients per cell, per time step. The computational cost being far higher, our implementation need to take this specificity into account. This is why we used an openCL mono-GPU implementation of Pn called "RKMS" (Reduced Kinetic Models Solver) `https://github.com/p-gerhard/rkms` developed locally by P. Gerhard for our implementation of both M1 and Pn. It is a very optimised code, which allows for very short computational times, but it is also not very flexible and adimensional, which led us to have to tinker with it a lot to implement our test cases and chemistry (see section 3).

2.2 High order and filtering

The results of Pn for a single continuous isotropic source shows us that it is almost equivalent to M1 in that specific case, which is promising. However, when we observe the results with two continuous isotropic sources, we observe that Pn does not show the pseudo-sources creation behaviour that M1 showcases, which means that Pn is able to correct that aspect of M1.

Other issues emerge when we leave the continuous isotropic regime. Indeed, Pn's closure relation makes it very sensible to discontinuous phenomena, causing oscillations and the apparition of modes. Worse, these oscillations can be negative, meaning we'd have the apparition of negative energy in these cases. Although Pn is mathematically correct, it does fail at correctly describing very discontinuous phenomena at a low order.

These issues becomes obvious when comparing the results of M1 and Pn for a non-continuous isotropic source. Here, our source is a simple impulsion, and while M1 responds quite well, Pn starts oscillating a lot. Increasing the order seems to limit the issue, but at the cost of a more expansive computational time. The other solution is to filter Pn which allows to greatly dampen the oscillations without increasing the computational cost, but it doesn't guarantee the positivity of the model. An mix of both methods is needed to ensure Pn obtains similar results to M1 in such cases.

Still, despite this apparent flaw, Pn corrects important issues of M1, and this becomes even more apparent in the last adimensional comparison we did, with continuous non-isotropic sources. Here, we have two sources generating directional energy beams which cross at the centre of our box as shown in fig.1. M1 fares very poorly in that test, as the two colliding wave front create a pseudo source changing the directionality of both beams. Once again, this issue is solved by Pn, despite the low intensity oscillations created by the discontinuity of non-isotropic sources.

3 Benchmarked Tests Cases

3.1 Chemistry

Chemistry implementation in RKMS required a lot of attention since it is a fully adimensional code. It is added to the code via a different kernel from the radiative transfer one, and based on tabulated chemistry values used in cosmological simulation code RAMSES (Teyssier 2002). To guarantee no negative energy enters the chemistry kernel and risks breaking it, since positivity energy w_0 can't be guaranteed, we decide to provide a modified version $w_0{}'$ of the energy to the chemistry kernel where we consider energy null in negative areas of w_0 (equ. 3.1). This modified energy is then used to update the ionised fraction which in turn generate a small variation of energy dw_0. This new variation is added back to the initial energy value w_0 of the radiative transfer kernel (equ. 3.2) to create a new initial energy condition for the next transfer time step $t+1$.

$$w_0^{t\,\prime} = max(w_0^t, 0) \tag{3.1}$$

$$w_0^{t+1} = w_0^t + dw_0^t \tag{3.2}$$

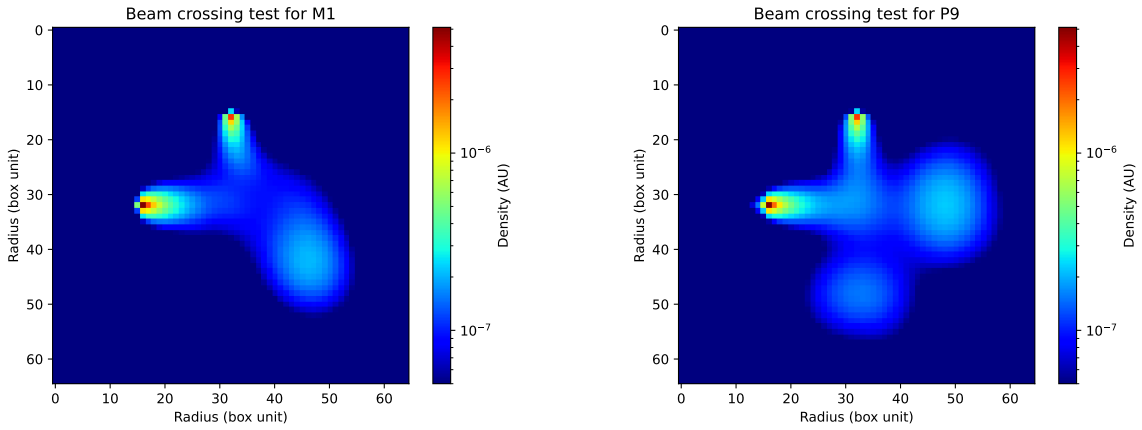

Fig. 1: Beam crossing test for M1 (left) and P9 (right). P9's oscillations have a lower density and aren't visible in this graph for the sake of comparison

3.2 Strömgren Sphere

The Strömgren Sphere test consists in observing the continuous regime of the sphere of ionised hydrogen surrounding a continuous isotropic source. Indeed, such a source should only be able to ionise gas in a sphere of radius R_s such as defined in 3.3 with $\dot{N}_\nu$ intensity of the source, $\alpha_B(T)$ recombination rate at a temperature T and n_H the hydrogen density. With this benchmark, we can easily confirm if our models is in accordance with the theoretical radius of the sphere.

$$R_s = \frac{3\dot{N}_\nu}{4\pi\alpha_B(T)n_H^2}^{1/3} \tag{3.3}$$

Two variations of the test case are made, one with a constant temperature of 100K (the isothermal case) and another one with temperature variation. In both situations, Pn matches the predictions and the results of M1 even at very low order (fig. 2).

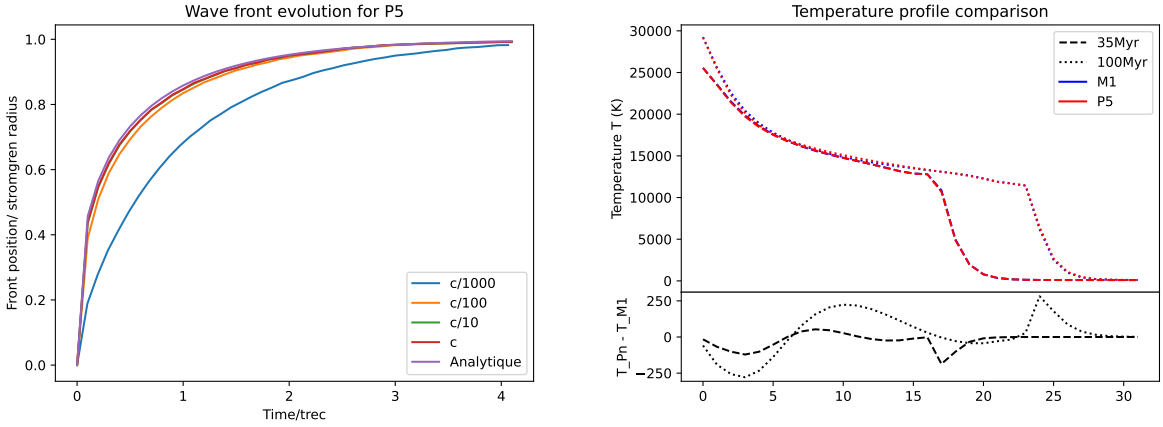

Fig. 2: **Left:** Ionisation front position of P5 compared to Strömgren Radius in isothermal case **Right:** Temperature profile comparison in Strömgren Sphere for non isothermal case

3.3 Shadowing a dense clump

This test consists in a very dense sphere of gas (referred as the "clump") in the path of a directive flux of photon. Such a dense region is expected to resist full ionisation and to slow down the ionisation rate in its wake.

This test is a bit trickier to implement with Pn due to some of the side effects of non-isotropic sources seen in section 2.2. The modes appearing around low order Pn sources make them less directive, and transparent boundary conditions can cause even more discontinuities in Pn, resulting in large and negative oscillations. All of these effects have to be taken into account to allow similar tests between M1 and Pn.

Once again, we can observe here that Pn have similar results to M1 at higher orders, even besting it in some aspects, especially the shadow of less ionised hydrogen in the clump's wake which is more visible in P9 than in M1, once again showcasing Pn's ability to correct M1 directionality issues. However, at low orders, we see oscillations and modes appearing, which is expected considering what we already talked about Pn in section 2.2.

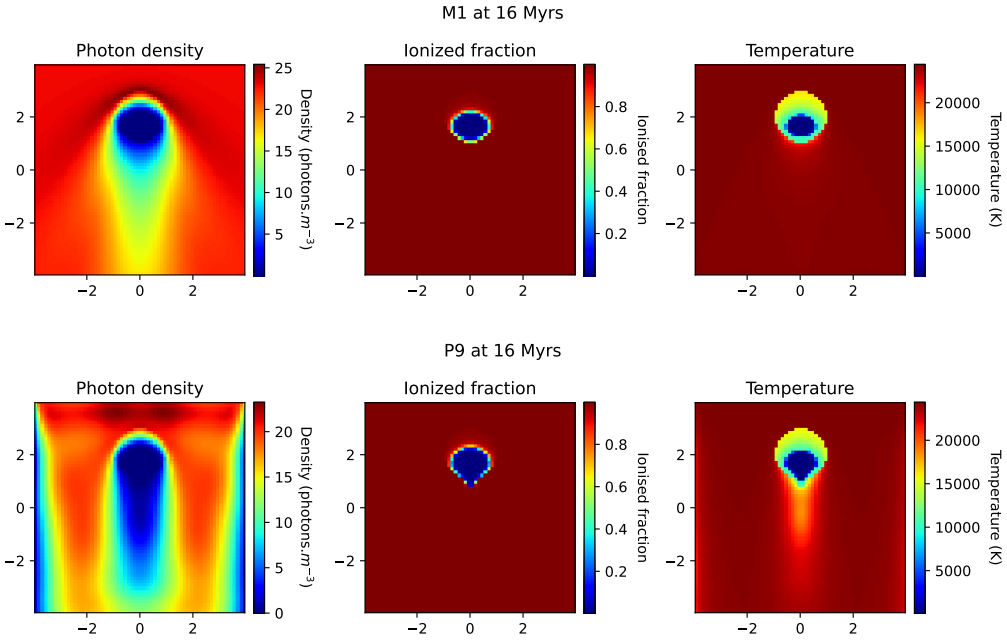

Fig. 3: Shadowing by a dense clump for M1 (top) and P9 (bottom). The photon flux flows from top to bottom.

4 Conclusions

In conclusion, we can safely say that Pn is a good alternative to M1, faring as well as it on most cases and correcting some of its flaws, especially the apparition of pseudo sources at the colliding point of two wave fronts, and the loss of directionality of M1. The next step would be for it to be implemented in a larger cosmological simulation code to see if the issues it solves from M1 have a larger impact on the results of the simulations and the observables of reionization, such as the statistics of the Lyman-α forest.

Thank you to Pierre Ocvirk and Emmanuel Franck, my PHD advisors, for their guidance in making a link between maths and astrophysics. A special thank also to Pierre Gerhard for his availability for tweaking RKMS to include our test cases.

References

Aubert, D. & Teyssier, R. 2008, Monthly Notices of the Royal Astronomical Society, 387, 295

Garrett, C. K. & Hauck, C. D. 2013, Transport Theory and Statistical Physics, 42, 203

Meltz, B. 2015, PhD thesis, University of Paris-Saclay, France

Teyssier, R. 2002, A&A, 385, 337

Wu, X., McQuinn, M., & Eisenstein, D. 2021, Journal of Cosmology and Astroparticle Physics, 2021, 042